

Mechanism of stress relaxation in (0001) InGaN/GaN via formation of V-shaped dislocation half-loops

A. V. Lobanova, A. L. Kolesnikova, A. E. Romanov, S. Yu. Karpov, M. E. Rudinsky et al.

Citation: *Appl. Phys. Lett.* **103**, 152106 (2013); doi: 10.1063/1.4824835

View online: <http://dx.doi.org/10.1063/1.4824835>

View Table of Contents: <http://apl.aip.org/resource/1/APPLAB/v103/i15>

Published by the [AIP Publishing LLC](#).

Additional information on *Appl. Phys. Lett.*

Journal Homepage: <http://apl.aip.org/>

Journal Information: http://apl.aip.org/about/about_the_journal

Top downloads: http://apl.aip.org/features/most_downloaded

Information for Authors: <http://apl.aip.org/authors>



PulseLine™ Ultrafast Laser Optics

The PulseLine family includes a number of standard, in-stock products which are ready to ship, and fully customized optics for volume applications

PULSELINE PRODUCTS

- MIRRORS
- BEAMSPLITTERS
- POLARIZING OPTICS (PLATES AND CUBES)
- PRISMS
- ANTI-REFLECTION WINDOWS

CVI Laser Optics
cvilaseroptics@idexcorp.com
cvilaseroptics.com

IDEX
OPTICS & PHOTONICS

ATFilms | Precision Photonics | CVI Laser Optics | Melles Griot | Semrock

Mechanism of stress relaxation in (0001) InGaN/GaN via formation of V-shaped dislocation half-loops

A. V. Lobanova,¹ A. L. Kolesnikova,² A. E. Romanov,³ S. Yu. Karpov,¹ M. E. Rudinsky,^{1,a)} and E. V. Yakovlev¹

¹STR Group–Soft-Impact Ltd., P.O. Box 83, 194156 St. Petersburg, Russia

²Institute of Problems of Mechanical Engineering RAS, 199178 St. Petersburg, Russia

³Ioffe Physical-Technical Institute RAS, 194021 St. Petersburg, Russia

(Received 19 July 2013; accepted 24 September 2013; published online 10 October 2013)

From the analysis of available experimental data, we suggest a mechanism of stress relaxation in strained (0001) InGaN/GaN layers, assuming formation of V-shaped edge-type dislocation half-loops. An energy-balance approach is applied to estimate the critical thickness of the InGaN layer resulting in generation of the V-shaped half-loops. The computed dependence of the critical thickness on the InGaN composition agrees well with the literature data reported for single-layer InGaN/GaN heterostructures. © 2013 AIP Publishing LLC. [<http://dx.doi.org/10.1063/1.4824835>]

Generally III-nitride heterostructures possess a large mismatch stress originated from the difference in the lattice parameters of binary compounds, GaN, AlN, and InN. The stress influences the indium incorporation in the InGaN alloys during their epitaxy, controls the bowing of the epitaxial wafers, and affects the band diagrams and polarization charge distributions in the grown structures.^{1,2} In turn, the stress relaxation produces extended defects that have a negative impact on the performance of the devices fabricated from such structures.^{3,4} Therefore, understanding of the relaxation mechanisms and conditions favorable for the relaxation onset is of primary importance for further development of III-nitride technology aimed at fabricating high-quality electronic and optoelectronic devices.

It is well known that generation of misfit dislocations (MDs) at {001}-type interface via dislocation gliding in {111}-type planes is the principal mechanism responsible for the stress relaxation in cubic III–V heterostructures.⁵ There exists a resolved shear stress in such glide planes and the relaxation starts as soon as the strained-layer thickness exceeds its critical value h_c that can be reasonably estimated from the Matthews-Blakeslee model.^{6,7} In contrast, III-nitride semiconductors have wurtzite crystal structure with the basal (0001) plane, being (i) most favorable for gliding of dislocations with the shortest Burgers vector $\mathbf{b} = a/3\langle 11\bar{2}0 \rangle$ (Ref. 8) and (ii) most frequently used for epitaxy of device structures. However, biaxial stress induced in a III-nitride heterostructure grown on the (0001) plane cannot provide dislocation gliding in the basal plane because of the absence of the resolved shear stress. This fact suggests the conventional mechanism of the interface MD formation due to dislocation easy-plane glide to be out of play in the (0001) InGaN/GaN structures. As a result, the stress relaxation in the InGaN layers is actually observed at the thicknesses much larger than h_c predicted by the Matthews-Blakeslee model.^{9,10} Attempts to consider alternative gliding systems, like prismatic $\langle 11\bar{2}3 \rangle\{11\bar{2}2\}$ ones possessing non-zero resolved shear stress, could not avoid the discrepancy between the theoretical predictions and available data.¹¹

We should also note that the data on h_c for the (0001) InGaN/GaN layers exhibit a large scatter of the reported values. On the one hand, this is related to variety of techniques used for identification of stress relaxation, including those providing indirect information (see below). On the other hand, h_c is frequently derived from the data reported by different groups and for the samples obtained under different conditions. Therefore, a careful selection of the data for comparison with theoretical predictions is a necessary step for validating models of stress relaxation.

In this paper, we report on the theoretical study of stress relaxation in (0001) InGaN/GaN layers. Based on literature data, we have identified the most typical features of this process and suggest a mechanism responsible for the stress relaxation in the above structures. Theoretical model corresponding to the suggested mechanism is applied to predict h_c of a single-layer InGaN/GaN heterostructure as a function of the alloy composition.

At the first stage of the study, we have selected reliable literature data on the stress relaxation in the (0001) InGaN/GaN structures. The relaxation is normally studied by various techniques, like transmission electron microscopy (TEM),^{12,13} atom probe tomography,¹⁴ luminescence measurements,^{15,16} etc. Most of them provide indirect information and does not allow unambiguous interpretation of the data obtained. In contrast, the X-ray diffraction reciprocal space mapping (XRD RSM)^{17–19} should especially be distinguished, as it delivers direct information on whether a particular InGaN layer is strained or partly/fully relaxed. The method is quite suitable for both bulk epitaxial layers and superlattices, while its applicability to single quantum wells (QWs) is limited only by sensitivity of the X-ray detector. We have chosen XRD RSM as a basic technique for examination of stress relaxation in InGaN layers and determination of their critical thicknesses.

Additional helpful information comes from TEM images where formation of dislocations in the InGaN is directly observable. Analysis of the TEM data has shown the stress relaxation in (0001) InGaN/GaN to be typically accompanied by formation of a sandwich-like structure including a sublayer adjacent to the underlying GaN with a

^{a)}Electronic mail: mikhail.rudinsky@str-soft.com

lower indium composition and an upper sublayer with higher indium content. Such a structure has been repeatedly reported for relatively thick InGaN layers (see, e.g., Refs. 14, 18, 20, and 21). The process is complicated by the development of surface roughness with subsequent tendency to faceting and composition fluctuations in the upper sublayer.^{18,20} A quite similar behavior was observed in compressively strained InAlN on GaN, also resulting in appearance of the sandwich-like structure.²²

Another important observation coming from TEM is that stress relaxation correlates with the formation of V-shaped edge-type dislocation half-loops (HLs) with the Burgers vector $\mathbf{b} = a/3\langle 11\bar{2}0 \rangle$.^{11,12,21,23–27} Such HLs (see Fig. 1) are formed within InGaN layer with their wings inclined from the c -axis toward one of the $\langle 1100 \rangle$ directions.²⁵ The opening angle of the HLs (2α) is found to vary in the range of $\sim 30^\circ$ – 50° , according to available observation. The HLs are observed in both bulk layers with relatively low indium composition^{21,26} and QWs of various compositions.^{23,26,27}

Experiments show that at high indium contents in InGaN layers, the density of the V-shaped dislocation HLs may be a few orders of magnitude higher than the threading dislocation density in the underlying GaN layer.^{24–26} Thus, one can conclude from the observations that the initial threading dislocations are not the major source of the dislocation HLs generated in InGaN during the stress relaxation. We assume the HLs to nucleate at the growth surface and then to climb presumably in the $\{11\bar{2}0\}$ -type planes down to the InGaN/GaN interface. The growth surface acts as a source of point defects necessary for dislocation climbing. As the wings of the HLs are inclined to the (0001) surface, they produce partial stress relaxation due to the presence of an effective MD component. This means that the mismatch stress in the InGaN layer is capable to produce the work required for the HL formation.

Based on the above consideration, we suggest the formation of V-shaped dislocation HLs to be the principal relaxation mechanism in the (0001) InGaN/GaN layers. The mechanism assumes growth of a strained layer up to the critical thickness above which the dislocation HLs start to appear. Here, the lateral stress arising from the lattice mismatch between InGaN and GaN is the driving force for the dislocation climb. The dislocation loops are produced until the stress in the InGaN layer is relieved partly or completely, and the stress relaxation provides a higher efficiency of

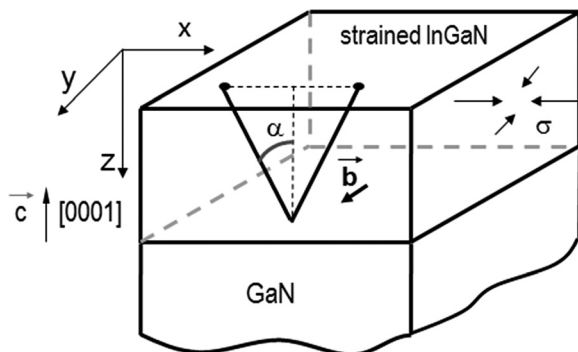


FIG. 1. Schematic view of a V-shaped edge-type dislocation half-loop with the Burgers vector \mathbf{b} .

indium incorporation for the further growth of InGaN.²⁸ As a result, an InGaN sublayer is formed with a higher composition on the top of the low-composition InGaN sublayer.

As soon as the dislocation HLs are formed, their elongation does no longer require consumption of point defects since it may occur just in course of epitaxial growth. If the angle α remains unchanged, like in the MQW structure covered by GaN,²⁴ the growth is expected to produce a continuously rising tensile strain in the subsequently grown InGaN or overgrown GaN/AlGaIn cap layer. The process of tensile stress appearance due to dislocation inclination was analyzed in Ref. 29. The strain evolution in the overgrown structures after the stress relaxation is, in our opinion, the subject for further experimental studies.

Appearance of a dislocation HL is frequently accompanied by the basal-plane stacking fault formation next to the apex of the loop.²⁶ In our opinion, this is the secondary process related to the stress concentration at the apex producing generation of new defects.

The critical thickness h_c for generation of the V-shaped dislocation loops has been estimated from the energy-balance approach similar to that used in Ref. 30 for the analysis of stress relaxation in AlGaIn layers by dislocation inclination. According to this approach, the energy release ΔE due to the V-shaped dislocation HL formation is

$$\Delta E = E_{\text{HL}} - \Delta W_{\text{int}}, \quad (1)$$

where E_{HL} is the self-energy of the dislocation HL, $\Delta W_{\text{int}} = b\sigma S$ is the energy release of the biaxial mismatch stress $\sigma = \sigma_{xx} = \sigma_{yy} = 2\mu\varepsilon_m(1+\nu)/(1-\nu)$ to produce the dislocation HL with the Burgers vector b and area S ; μ is the shear modulus, ν is the Poisson ratio, $\varepsilon_m = (a_{\text{InGaIn}} - a_{\text{GaN}})/a_{\text{InGaIn}}$ is the misfit strain, while a_{InGaIn} and a_{GaN} are the lattice constants of the InGaIn and underlying GaN, respectively.

To evaluate the elastic energy, we use the isotropic-media approximation. The elastic field of the dislocation half-loop is found by integration of the fields of infinitesimal prismatic dislocation loops (IPDLs) over the total HL area S_{HL} (Ref. 31)

$$\sigma_{ij}(x, y, z) = \int_{S_{\text{HL}}} \sigma_{ij}^{\text{IPDL}}(x, y, z; x', 0, z') \rho \, dx' dz', \quad (2)$$

where $\sigma_{ij}^{\text{IPDL}}$ are the components of the stress tensor of a single IPDL in a half space, $(x', 0, z')$ are the coordinates of the IPDL, $\rho = 1/\Delta S$ is the density of the IPDLs, and ΔS is the area of the single IPDL. The elastic self-energy E_{HL} is then determined by a proper integrating of the HL elastic field. Numerical solution of the equation $\Delta E = 0$ provides the critical thickness h_c .

The Poisson ratio ν is averaged over all the directions in the wurtzite crystal.³² Variation of the Poisson ratio with the layer composition appears to have a negligible effect on the overall result, thus, we have taken $\nu = 0.24$, corresponding to the InN molar fraction of 0.1. The dislocation core radius R_c , accounting indirectly for the core energy in a conventional way, is chosen to be equal to $b/2$, as this value has been proved to provide quite reasonable predictions for semipolar

and nonpolar III-nitrides structures.³² The opening angle 2α remains a free parameter in our model to be determined from experiments.

Figure 2 compares the computed h_c as a function of InGaN composition with the data obtained by the most informative characterization techniques described above. Here, most of the experimental have been selected by satisfying two criteria: (i) observation of a transition from stressed to relaxed state of InGaN confirmed by XRD RSM and (ii) observation of extra V-shaped edge-type dislocation HLs confirmed by TEM. The InGaN composition of the sample studied in Ref. 23 was corrected by comparison of its emission spectrum with those reported in Ref. 24 for the samples with well-known compositions. We also add to Fig. 2 the data by Reed *et al.*¹⁵ obtained by luminescence technique, as they cover the low-composition region and are consistent with other measurements in the middle-composition region. The computational results corresponding to variation of the angle α from 15° to 25° are shown in Fig. 2 by the gray shadow. The model provides quite reasonable agreement with the measurements in the range of the $\text{In}_x\text{Ga}_{1-x}\text{N}$ composition $x \sim 0.15$ – 0.30 , while the experimental h_c are larger than the computed ones by a factor of ~ 1.3 – 2.0 at $x < 0.15$. The above discrepancy can be attributed in part to neglecting interference of the elastic fields of the neighboring HLs that start to intersect with each other in thick InGaN layers.

Computations for $x > 0.3$ are also possible but require selecting another R_c value, different from the presently used $b/2$, since the solution to the equation $\Delta E = 0$ does not exist at the chosen core radius. At $x > 0.3$, both the theory and available data predict h_c to be less than ~ 2 – 3 nm, which are typical widths of the QWs emitting green light. This means that the strained InGaN QWs may become unstable at such InGaN compositions. To understand better the stability of strained InGaN/GaN layers at high InGaN compositions, atomistic simulations would be helpful.

The nature of HL opening and the factors that may affect the value of the opening angle still remains obscure. By now, we could not find from the reported data any correlation between the angle, parameters of the InGaN layer (composition and thickness), and its growth conditions (temperature, growth rate, etc.). So, further in-deep analysis,

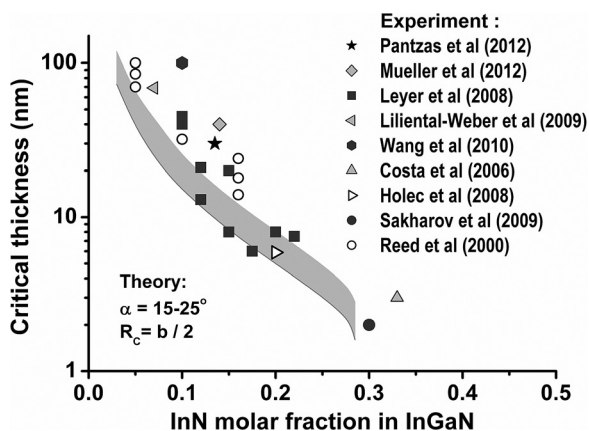


FIG. 2. Critical thickness versus InGaN composition: gray shadow indicates theoretical predictions for $R_c = b/2$ and angle α varied from 15° to 25° , symbols are the experimental data from different papers.

involving existing and newly appearing experimental information, is required to establish possible correlations. One more question for the further analysis is whether the $\{11\bar{2}0\}$ -type planes are the unique ones for the climb of the V-shaped HLs or other planes may be involved, too.

To conclude, we have suggested a mechanism of stress relaxation in (0001) InGaN/GaN heterostructures via formation of V-shaped edge-type dislocation HLs. This mechanism is consistent with the main experimental findings demonstrating, in particular, that (i) such HLs are generated at the growth surface and frequently penetrate down to the InGaN/GaN interface, as shown by TEM, (ii) they are responsible for the stress relaxation, as demonstrated by XRD RSM, and (iii) they have the Burgers vector $\mathbf{b} = a/3\langle 11\bar{2}0 \rangle$ as it follows from TEM. In contrast to the conventional mechanism of stress relaxation assuming the interface MD formation, the suggested mechanism implies a feasible non-zero resolved normal stress to provide the climb of the HLs in the m-plane of the wurtzite crystal. Since the climb requires consumption of point defects that may come from the growth surface, the stress relaxation is expected to be enhanced at high InGaN growth temperatures.

Calculations of the critical thicknesses of InGaN layers corresponding to the V-shaped HL formation have been carried out by using the energy-balance approach. The dependence of h_c on the InGaN composition obtained in such a way is in reasonable agreement with the selected data reported for single layers of various compositions.

Among the model applications, we can outline both predictive determination of the critical thicknesses that would enable more accurate design of green-light emitters free of stress relaxation and modeling of thick InGaN epitaxial growth with the account of possible stress relaxation.

A.L.K. and A.E.R. were in part supported by RFBR Project No. 12-08-00397a.

¹J. H. Ryou, P. D. Yoder, J. P. Liu, Z. Lochner, H. Kim, S. Choi, H. J. Kim, and R. D. Dupuis, *IEEE J. Sel. Top. Quantum Electron.* **15**(4), 1080 (2009).

²M. E. Aumer, S. F. LeBoeuf, B. F. Moody, and S. M. Bedair, *Appl. Phys. Lett.* **79**, 3803 (2001).

³X.-A. Cao, in *GaN and ZnO-based Materials and Devices*, edited by S. Pearton (Springer, New York, 2012), Chap. 4.

⁴K.-S. Lee, Isnaeni, Y.-S. Yoo, J.-H. Lee, Y.-C. Kim, and Y.-H. Cho, *J. Appl. Phys.* **113**, 173512 (2013).

⁵J. Tsao, *Materials Fundamentals of Molecular Beam Epitaxy* (Academic Press, Inc., San Diego, CA, 1993), Chap. 5.

⁶J. W. Matthews and A. E. Blakeslee, *J. Cryst. Growth* **27**, 118 (1974).

⁷L. B. Freund, *J. Appl. Mech.* **54**, 553 (1987).

⁸Y. A. Osipyan and I. S. Smirnova, *Phys. Status Solidi* **30**, 19 (1968).

⁹I. Akasaki and H. Amano, *Jpn. J. Appl. Phys., Part 1* **36**, 5393 (1997).

¹⁰D. Holec, P. M. F. J. Costa, M. J. Kappers, and C. J. Humphreys, *J. Cryst. Growth* **303**, 314 (2007).

¹¹D. Holec, Y. Zhang, D. V. Sridhara Rao, M. J. Kappers, C. McAleese, and C. J. Humphreys, *J. Appl. Phys.* **104**, 123514 (2008).

¹²W. Lu, D. B. Li, C. R. Li, F. Shen, and Z. Zhang, *J. Appl. Phys.* **95**, 4362 (2004).

¹³S. Srinivasan, L. Geng, R. Liu, F. A. Ponce, Y. Narukawa, and S. Tanaka, *Appl. Phys. Lett.* **83**, 5187 (2003).

¹⁴M. Müller, G. D. W. Smith, B. Gault, and C. R. M. Grover, *Acta Mater.* **60**, 4277 (2012).

¹⁵M. J. Reed, N. A. El-Masry, C. A. Parker, J. C. Roberts, and S. M. Bedair, *Appl. Phys. Lett.* **77**, 4121 (2000).

- ¹⁶A. M. Emara, E. A. Berkman, J. Zavada, N. A. El-Masry, and S. M. Bedair, *Phys. Status Solidi C* **8**, 2034 (2011).
- ¹⁷S. Pereira, M. R. Correia, E. Pereira, K. P. O'Donnell, E. Alves, A. D. Sequeira, N. Franco, I. M. Watson, and C. J. Deatcher, *Appl. Phys. Lett.* **80**, 3913 (2002).
- ¹⁸K. Pantzas, G. Patriarche, G. Orsal, S. Gautier, T. Moudakir, M. Abid, V. Gorge, Z. Djebbour, P. L. Voss, and A. Ougazzaden, *Phys. Status Solidi A* **209**, 25 (2012).
- ¹⁹M. Leyer, J. Stellmach, Ch. Meissner, M. Pristovsek, and M. Kneissl, *J. Cryst. Growth* **310**, 4913 (2008).
- ²⁰Z. Liliental-Weber, K. M. Yu, M. Hawkrige, S. Bedair, A. E. Berman, A. Emara, D. R. Khanal, J. Wu, J. Domagala, and J. Bak-Misiuk, *Phys. Status Solidi C* **6**, 2626 (2009).
- ²¹H. Wang, D. S. Jiang, U. Jahn, J. J. Zhu, D. G. Zhao, Z. S. Liu, S. M. Zhang, Y. X. Qiu, and H. Yang, *Physica B* **405**, 4668 (2010).
- ²²Z. T. Chen, K. Fujita, J. Ichikawa, and T. Egawa, *J. Appl. Phys.* **111**, 053535 (2012).
- ²³P. M. F. J. Costa, R. Datta, M. J. Kappers, M. E. Vickers, C. J. Humphreys, D. M. Graham, P. Dawson, M. J. Godfrey, E. J. Thrush, and J. T. Mullins, *Phys. Status Solidi A* **203**, 1729 (2006).
- ²⁴A. V. Sakharov, W. V. Lundin, E. E. Zavarin, M. A. Sinitsyn, A. E. Nikolaev, S. O. Usov, V. S. Sizov, G. A. Mikhailovsky, N. A. Cherkashin, M. Hytch, F. Hue, E. V. Yakovlev, A. V. Lobanova, and A. F. Tsatsulnikov, *Semiconductors* **43**, 812 (2009).
- ²⁵M. Zhu, S. You, T. Detchprohm, T. Paskova, E. A. Preble, D. Hanser, and C. Wetzel, *Phys. Rev. B* **81**, 125325 (2010).
- ²⁶F. Y. Meng, H. McFelea, R. Datta, U. Choudhury, C. Werkhoven, C. Arena, and S. Mahajan, *J. Appl. Phys.* **110**, 073503 (2011).
- ²⁷U. Strauss, T. Lerner, J. Muller, T. Hager, G. Bruderl, A. Avramescu, A. Lell, and C. Eichler, *Phys. Status Solidi A* **209**, 481 (2012).
- ²⁸S. Yu. Karpov, R. A. Talalaev, E. V. Yakovlev, and Yu. N. Makarov, *MRS Proceedings* **639**, G3.18 (2000).
- ²⁹A. E. Romanov, G. E. Beltz, and J. S. Speck, *Int. J. Mater. Res.* **98**, 723–728 (2007).
- ³⁰P. Cantu, F. Wu, S. Keller, A. E. Romanov, S. P. DenBaars, and J. S. Speck, *J. Appl. Phys.* **97**, 103534 (2005).
- ³¹P. P. Groves and D. J. Bacon, *Philos. Mag.* **22**, 83 (1970).
- ³²A. E. Romanov, E. C. Young, F. Wu, A. Tyagi, C. S. Gallinat, S. Nakamura, S. P. DenBaars, and J. S. Speck, *J. Appl. Phys.* **109**, 103522 (2011).